International Journal of Heat and Technology
Vol. 42, No. 3, June, 2024, pp. 1021-1028
Journal homepage: http://iieta.org/journals/ijht

Thermodynamic Foundations of Intelligent Algorithms for Enhancing Efficiency in Industrial Thermal Processes

Jian Dong

School of Intelligent Manufacturing, Zibo Vocational Institute, Zibo 255000, China

Corresponding Author Email: 12070@zbvc.edu.cn

https://doi.org/10.18280/ijht.420329

Received: 10 December 2023
Revised: 16 April 2024
Accepted: 13 May 2024
Available online: 27 June 2024

Keywords:
industrial thermal processes, thermal efficiency, intelligent algorithms, thermodynamic fundamentals, mathematical model, optimized Gaussian process regression, prediction and optimization

ABSTRACT

Industrial thermal processes are pivotal in modern industrial production, significantly impacting energy utilization and production costs. With the growing scarcity of global energy resources and heightened environmental protection standards, enhancing the thermal efficiency of industrial processes has become a research focus. Intelligent algorithms offer a novel approach to this challenge by integrating thermodynamic principles with optimization techniques, enabling precise modeling and efficient optimization of complex thermal processes. However, traditional mathematical models and optimization algorithms still lack in complexity, efficiency, and accuracy. This paper proposes a systematic research framework grounded in thermodynamic fundamentals. The study comprises two main parts: firstly, establishing a comprehensive mathematical model of industrial thermal process efficiency that incorporates various thermodynamic factors and process parameters; secondly, employing an optimized Gaussian process regression method for predicting and optimizing thermal efficiency. This research not only enriches the theoretical foundation of industrial thermal process optimization but also provides scientific guidance and technical support for practical applications, enhancing energy utilization and reducing production costs.

1. INTRODUCTION

Industrial thermal processes are crucial components of modern industrial production, with their efficiency directly impacting energy utilization and production costs [1-3]. As global energy resources become increasingly scarce and environmental protection requirements continue to rise, improving the thermal efficiency of industrial processes has become a focus of attention for both academia and industry [4-6]. Traditional methods of managing industrial thermal processes rely on experience and qualitative analysis, lacking systematic theoretical guidance and quantitative models, making precise control and optimization difficult.

The introduction of intelligent algorithms provides new thoughts and methods for addressing the efficiency issues of industrial thermal processes. By integrating thermodynamic principles with modern optimization techniques, intelligent algorithms can accurately model and efficiently optimize complex thermal processes, significantly enhancing thermal efficiency and energy utilization [7-11]. Furthermore, intelligent algorithms also enable real-time monitoring and dynamic adjustments, offering more flexible and efficient solutions for industrial production [12, 13]. Therefore, studying the thermodynamic foundations of intelligent algorithms in enhancing the efficiency of industrial thermal processes is of significant theoretical and practical importance.

Although existing research has made some progress in modeling and optimizing industrial thermal processes, there are still several deficiencies. Firstly, traditional mathematical models often oversimplify and fail to fully reflect the complexity and dynamics of actual industrial thermal processes [14-16]. Secondly, some optimization algorithms are inefficient when dealing with large-scale and high-dimensional data, failing to meet the demands of practical applications [17-19]. Additionally, existing prediction models still need improvements in accuracy and robustness, particularly in handling multivariable couplings and nonlinear relationships.

This paper examines how intelligent algorithms can boost the efficiency of industrial thermal processes through advanced thermodynamic analysis. It is structured in two parts: initially, we develop a mathematical model for thermal efficiency that incorporates various thermodynamic and process variables. Subsequently, we use optimized Gaussian process regression to predict and enhance this efficiency, suggesting practical improvements. This research deepens the theoretical understanding of industrial thermal optimization and offers valuable insights for enhancing energy efficiency and lowering production costs, presenting substantial academic and practical benefits.

2. MATHEMATICAL MODELING OF INDUSTRIAL THERMAL EFFICIENCY

In industrial thermal processes, enhancing thermal efficiency is crucial for improving energy utilization and reducing production costs. Figure 1 shows the control strategies for industrial thermal processes. Establishing a mathematical model of industrial thermal process efficiency is a necessary step to achieve this goal. Mathematical modeling allows for the quantitative analysis of complex thermal processes and reveals the interactions between various thermodynamic factors and process parameters, providing a scientific basis for optimization control.

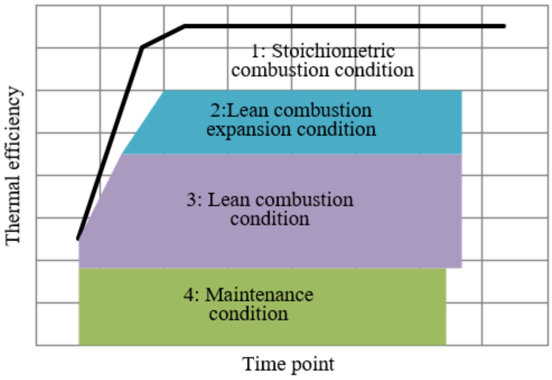

Figure 1. Industrial thermal process control strategies

In developing the mathematical model for the efficiency of industrial thermal processes, it is necessary to consider five key aspects: total thermal efficiency of the heat source, exhaust gas heat loss, incomplete chemical combustion heat loss, incomplete mechanical combustion heat loss, radiative heat loss, and sensible heat loss from slag. Specifically, this paper defines the total thermal efficiency of the heat source using Eq. (1) as follows. The total thermal efficiency of the heat source measures the efficiency of converting energy input into effective thermal energy. This step involves determining the ratio of input thermal energy to output effective thermal energy, establishing an energy balance equation for the heat source. By analyzing the heat source system and considering various influencing factors such as fuel type, combustion temperature, and pressure, the total thermal efficiency of the heat source is accurately calculated. Assuming that the net heat absorption is represented by w_1, exhaust gas heat loss by w_2, incomplete chemical combustion heat loss by w_3, incomplete mechanical combustion heat loss by w_4, radiative heat loss by w_5, and sensible heat loss from slag by w_6, the mathematical expression is:

$$\lambda_{hm} = w_1 = 100 - \sum_{u=2}^{6} w_u \tag{1}$$

Exhaust gas heat loss refers to the heat carried away by the flue gases generated during combustion. To accurately estimate exhaust gas heat loss, it is necessary to measure the temperature, flow rate, and composition of the flue gases, and calculate the total heat carried by the flue gases using thermodynamic formulas. The mathematical model for exhaust gas heat loss includes both sensible and latent heat losses. Assuming the excess air coefficient at the exhaust is represented by β_{ob}, exhaust temperature by ϕ_{ob}, and ambient temperature by s_{AM}, then the formula is:

$$w_2 = \left(l + v\beta_{ob}\right)\left(1 - \frac{w_4}{100}\right)\frac{\varphi_{ob} - s_{AM}}{100} \tag{2}$$

Incomplete chemical combustion heat loss occurs due to the incomplete combustion of combustible components in the fuel. It is necessary to determine the unburned components and their quantities through stoichiometric and combustion analysis. Then, using thermochemical formulas, the heat value of the unburned components is calculated, establishing the corresponding mathematical model. Assuming the volume fractions of O_2 and CO at the flue measurement point are represented by N_{P2} and N_{ZP}, $\beta \approx 0.21/(0.21 - N_{P2})$, $\eta = 3.2$, then the formula is:

$$w_3 = \eta \beta N_{ZP} \tag{3}$$

Incomplete mechanical combustion heat loss refers to the heat loss caused by unburned fuel residues in the mechanical system due to incomplete combustion. This step requires fuel analysis and combustion tests to measure the quantity and composition of the residual fuels, combined with the operating parameters of the mechanical system, to calculate the heat loss due to incomplete mechanical combustion. Assuming the percentage of ash content in the fuel is represented by X_{xe}, the lower heating value of the fuel by W_e, the percentage of combustibles in ash and fly ash by Z_{gc} and Z_{dg}, and the proportion of ash and fly ash in the fuel by β_{gc} and β_{dg}, then the expression is:

$$w_4 = \frac{YX_{xe}}{W_e}\left(\frac{\beta_{gc} Z_{gc}}{100 - Z_{gc}} + \frac{\beta_{dg} Z_{dg}}{100 - Z_{dg}}\right) \tag{4}$$

Radiative heat loss refers to the heat dissipated to the environment through conduction, convection, and radiation during the thermal process. To accurately estimate radiative heat loss, it is necessary to measure the temperature and heat flux density on the surface of the thermal equipment, considering the material properties of the equipment and environmental conditions, and calculate the heat dissipation using heat transfer formulas. The mathematical model constructed for radiative heat loss includes a detailed analysis of each heat dissipation path. Assuming that the radiative heat loss at the rated evaporation or heating capacity is represented by w'_5, the current operating load of the heat source by A, and the rated load of the heat source by A_0, the expression for radiative heat loss is:

$$w_5 = w'_5 \frac{A}{A_0} \tag{5}$$

Sensible heat loss from slag refers to the heat carried by the slag after combustion. By measuring the temperature and mass of the slag and combining it with its specific heat capacity, the sensible heat of the slag is calculated. The mathematical model for sensible heat loss from slag includes a detailed analysis of the slag's composition and thermal properties. Assuming the enthalpy of slag is represented by $(zn)_{gc}$, the expression is:

$$w_6 = \beta_{gc} \frac{100}{100 - Z_{gc}} (zn)_{gc} \frac{X_{xe}}{W_e} \tag{6}$$

$(zn)_{gc}$ can be fitted by the following formula:

$$(zn)_{gc} = 0.0002887\varphi_{ob}^2 + 0.6851\varphi_{ob} + 26.76 \tag{7}$$

3. OPTIMIZING THERMAL EFFICIENCY WITH GAUSSIAN PROCESS REGRESSION

3.1 Gaussian process regression

In the study of the thermal efficiency of industrial thermal processes, due to the limited number of data samples and the high-dimensionality and non-linearity of the data, choosing an appropriate regression method for prediction and optimization is particularly important. Gaussian process regression has strong generalization capabilities and can provide reliable predictions by combining prior knowledge and observed data, even in cases of small samples. Given the potential complex non-linear relationships among multiple influencing factors in the data of industrial thermal processes, Gaussian process regression defines a kernel function in the input space to accurately capture the non-linear relationships among input variables, further providing precise predictions. Additionally, the Gaussian process regression model has adaptive characteristics, allowing it to automatically adjust the complexity of the model based on the characteristics of the data, ensuring the accuracy and robustness of the predictions. Figure 2 provides a flowchart of the industrial thermal process efficiency prediction model based on Gaussian process regression.

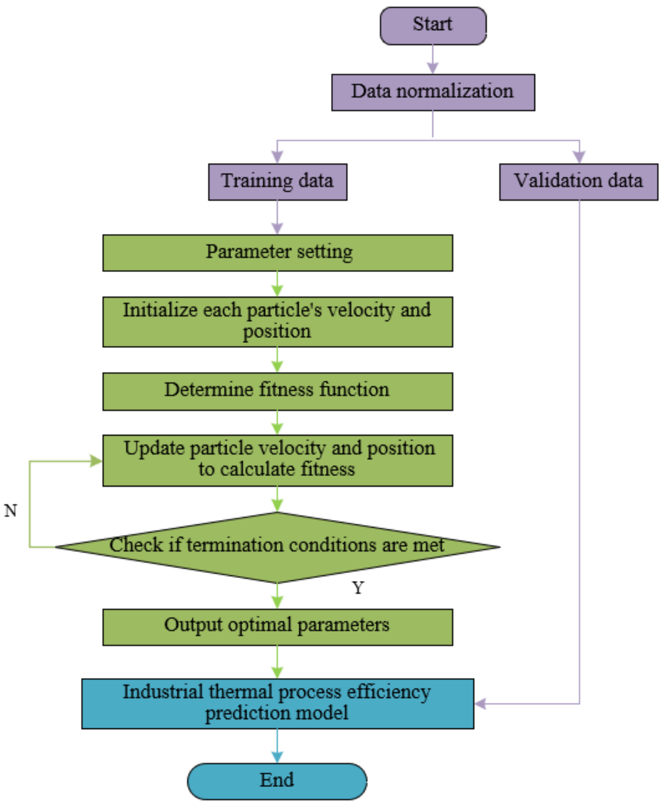

Figure 2. Flowchart of industrial thermal process efficiency prediction model based on Gaussian process regression

Initially, this paper collected relevant data from actual industrial production processes to construct a comprehensive training dataset. These data include various input variables affecting thermal efficiency, such as temperature, pressure, fuel type, flow rate, and equipment status, which should comprehensively reflect the various operating conditions in industrial thermal processes. Additionally, corresponding output data, namely the thermal efficiency under each operating condition, must also be recorded. Constructing the dataset requires not only ensuring the accuracy and completeness of the data but also paying attention to data preprocessing, such as removing outliers, filling missing values, and normalization, to improve data quality and model training effectiveness. Specifically, the training dataset is constructed as $F=\{(a_u,b_u)|u=1,2,3,\ldots,v\}=\{(A,b)\}$, where a_u represents the u-th input vector, containing various influencing factors in industrial thermal processes, and b_u represents the corresponding output thermal efficiency data. This dataset forms the basis for model training.

Next, the objective function $d(a)$ is defined, representing the thermal efficiency corresponding to the input vector a, to describe the relationship between the input variables and thermal efficiency. The sample set input matrix corresponding to A is denoted by A', and the Gaussian process assumes that the target function $d(a)$ follows a joint Gaussian distribution, with its statistical characteristics determined by the mean function $l(A)$ and the covariance function $J(A, A')$. The mean function $l(A)$ is typically set to zero mean, and the covariance function $J(A, A')$ uses a squared exponential function form. Assuming Gaussian white noise is represented by γ, the Gaussian process probability function HO can be expressed as:

$$d(a) \sim HO\left(l(A), J(A, A')\right) \tag{8}$$

$$b = d(a) + \gamma \tag{9}$$

Assuming the v-th order covariance matrix is represented by $J(A,A)+\delta^2_v U$, and the v-th order kernel matrix by $J(A, A)=(j_{uk})$, where the matrix elements $j_{uk}=j(a_u, a_k)$, the prior distribution of b can be represented as:

$$b \sim HO\left(l(A), J(A, A)+\delta_v^2 U\right) \tag{10}$$

Then, using the Bayesian framework, the joint Gaussian distribution of the target outputs b and the validation dataset target outputs b^* is calculated based on the prior distribution and the likelihood function, deriving the posterior distribution of the validation dataset $F_*=\{(A_*,b_*)\}$. For a given training set (X, y) and test set A_*, the posterior probability distribution can be represented as: $b_*|A_*,A,b \sim N(\mu_*,\Phi_*)$, where μ^* and Φ^* respectively represent the posterior mean and covariance matrix. Assuming the $v\times1$ order covariance matrix between the training data A and the validation data X_* is represented by $J(A, A_*)=J(A_*, A)^S$, and the covariance of the validation point a^* itself by $j(A^*, A^*)$, the joint Gaussian distribution of b and b_* is calculated using the following formula:

$$\begin{bmatrix} b \\ b_* \end{bmatrix} = \left(0, \begin{bmatrix} J(A,A)+\delta_v^2 U & J(A,A_*) \\ J(A_*,A) & J(A_*,A_*) \end{bmatrix}\right) \tag{11}$$

To further optimize the model, appropriate kernel function parameters need to be selected. By maximizing the likelihood function or using cross-validation methods, the best parameter combinations can be determined to improve the model's prediction accuracy and stability. Finally, the trained model is applied to the prediction and optimization of industrial thermal process efficiency. Assuming the expected value following a standard normal distribution is represented by $\bar{b}_*$, the expectation function by $R(\cdot)$, and $COV(b_*)$ as the variance, the posterior probability distribution of b_* can be represented as:

$$b_*|A,b,A_* \sim V\left(\bar{b}_*, COV(b_*)\right) \tag{12}$$

$$\bar{b}_* = R\left(b_*|A,b,A_*\right) = J(a_*,a)\left[J(A,A)+\delta_v^2 U\right]^{-1} b \tag{13}$$

$$\begin{aligned} COV(b_*) &= j(A_*,A_*) \\ &-J(A_*,A_*)\left[J(A,A)+\delta_v^2 U\right]^{-1} J(A,A_*) \end{aligned} \tag{14}$$

Assuming the variance scale is represented by m, and δ^2_d is the signal variance of the kernel function, then the covariance kernel function expression is:

$$j(a_u,a_k) = \delta_d^2 \exp\left[\frac{-(a_u-a_k)^2}{2m^2}\right] \tag{15}$$

The trained model is then applied to the actual prediction and optimization of industrial thermal process efficiency. Based on the model's prediction results, the impact of each input factor on thermal efficiency is analyzed, identifying key factors and optimal operating conditions. Combining thermodynamic principles and practical production experience, improvement measures and optimization strategies are proposed, such as adjusting process parameters, optimizing equipment operation, improving fuel mix, etc. Through continuous iteration and optimization, the goals of efficient operation and energy-saving emission reduction of industrial thermal processes are achieved.

3.2 Particle Swarm Optimization (PSO) for Gaussian process regression

In the modeling and prediction of industrial thermal processes, thermal efficiency is influenced by multiple complex factors, including temperature, pressure, fuel type, etc. The Gaussian process regression model captures the nonlinear relationships between input variables through the covariance function, but accurate predictions require the selection of appropriate hyperparameters. The PSO algorithm, through collective intelligence and iterative optimization, can find a set of hyperparameters that minimize the error of the Gaussian process regression model while ensuring prediction accuracy, thereby enhancing the model's predictive performance.

The specific steps for optimizing the Gaussian process regression model using the PSO are as follows:

Step 1: Set initial PSO parameters

First, set the initial parameters of the PSO algorithm. These parameters include setting the population size N=20, spatial dimension D=3, inertia coefficient w=1, acceleration constants $c1$=$c2$=1.5, and a maximum of 300 iterations. The velocity control range for the particles in the three dimensions corresponds to the range of values for the model's three hyperparameters $\phi=\{\delta^2_v, \delta^2_d, m\}$, set to [-1, +1], [-100, +100], [-10, +10], respectively.

Step 2: Initialize PSO parameters

In the F-dimensional space, randomly initialize the parameters of the particle swarm, including each particle's initial position a_u and velocity n_u. These initial values should be within the set range to ensure that the swarm can fully explore the entire search space to find the optimal combination of hyperparameters. Further define the PSO's fitness function, used to evaluate each particle's performance. The fitness function is typically related to the *GPR* model's prediction error, specifically, the mean squared error can be used as the evaluation standard for the fitness function. Calculate the fitness value of each particle in its current state to determine its performance in the search space. Assuming the total number of training data is represented by v; actual output by b^u_*; predicted output by b^{-u}_*, the expression is:

$$FIT(a) = \frac{1}{v}\sum_{u=1}^{v}\left(b_*^u - \bar{b}_*^u\right)^2 \tag{16}$$

Step 3: Iteratively update particle parameters

According to the PSO's updating rules, iteratively update each particle's parameters. During the updating process, each particle's velocity and position are adjusted according to its own best position and the global best position. This method ensures that particles can explore new areas while leveraging existing good solutions, gradually approaching the optimal solution. In each iteration, recalculate each particle's fitness value and update the global and local best solutions. Assuming the spatial dimension is represented by f, the u-th particle's position velocity and individual best solution by A^j_{uf}, N^{j+1}_{uf}, O^j_{uf}, and the global best solution by O^j_{hf}, random numbers by e_1 and e_2, the formulas are:

$$\begin{cases} N_{uf}^{j+1} = qN_{uf}^j + z_1 e_1\left(O_{uf}^j - A_{uf}^j\right) + z_2 e_2\left(O_{hf}^j - A_{uf}^j\right) \\ A_{uf}^{j+1} = A_{uf}^j + N_{uf}^{j+1} \end{cases} \tag{17}$$

Step 4: Termination condition check

Check if the termination conditions are met. The termination condition can be reaching the maximum number of iterations, or the change in the global best solution being below a certain threshold over several consecutive iterations. If the termination conditions are met, end the optimization process and output the model's optimal hyperparameters $\phi=\{\delta^2_v, \delta^2_d, m\}$. Otherwise, return to Step 3 to continue iteratively updating the particle parameters.

Through the optimized model, key parameters in the industrial thermal process are monitored and predicted in real-time. Figure 3 shows the schematic diagram of the thermal efficiency testing system. The model can accurately predict the trend of system thermal efficiency changes based on the input real-time data, identifying the main factors and parameter combinations that affect thermal efficiency. Then, based on these predictive results, data-driven analysis and diagnostics can be conducted to identify bottlenecks and potential improvement areas in system operation. Once accurate thermal efficiency predictions are obtained, the next step is to develop optimization strategies. This specifically includes adjusting process parameters and operating conditions to achieve optimal thermal efficiency. For example, based on the model's predictive results, adjustments might be made to the fuel supply and air flow ratio of burners, optimization of the operating parameters of heat exchangers, and adjustments to the operating temperature and pressure of reactors. These adjustments need to be repeatedly validated in conjunction with practical operational experience and model predictions to ensure that thermal efficiency is maximized without affecting production safety and product quality.

Furthermore, based on the model's predictive results, preventive maintenance and intelligent scheduling can also be implemented. By predicting changes in equipment operation status and thermal efficiency, potential faults and performance degradations can be identified in advance, allowing for timely maintenance and replacement to avoid increased energy consumption and production interruptions caused by equipment failures. At the same time, production scheduling can be optimized, arranging production plans rationally to avoid unnecessary waste of energy.

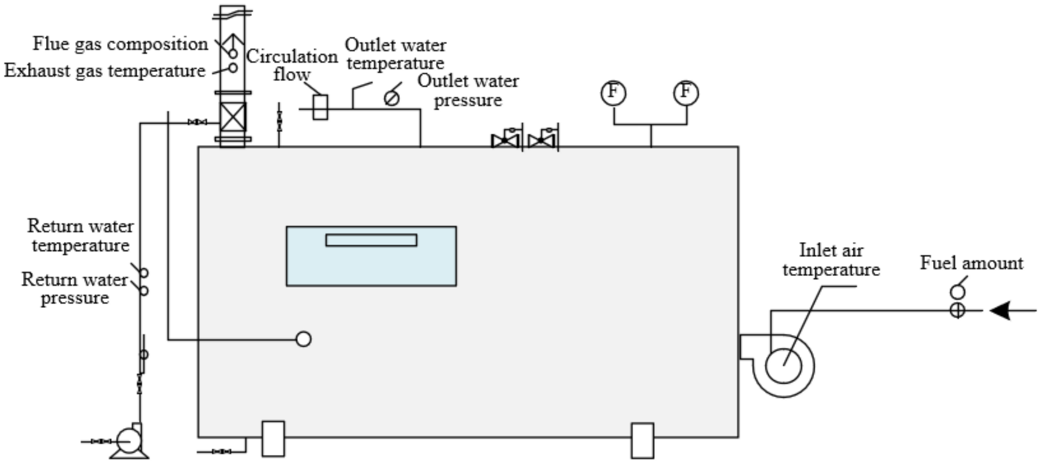

Figure 3. Schematic diagram of the thermal efficiency testing system

4. EXPERIMENTAL RESULTS AND ANALYSIS

In Figure 4, the fitness of the PSO-optimized Gaussian process regression algorithm initially decreases sharply, falling from 0.104 at the start to 0.0799 by the 50th generation. This trend of decline slows after the initial drop, stabilizing and reaching a minimum of 0.0713 near the 200th generation. The trend of the average fitness is similar to that of the best fitness, showing a steady decrease, especially within the first 100 generations, gradually decreasing from 0.0747 to 0.0677. After 200 generations, although both the best and average fitness levels fluctuate, the overall trend tends to stabilize, indicating that the algorithm has found a relatively stable optimized solution after a certain number of iterations. The analysis of the experimental data shows that the proposed algorithm demonstrated high adaptability in optimizing the efficiency of industrial thermal processes, particularly in the early stages of iteration. The significant drop in fitness early on indicates that the algorithm quickly found a superior solution and further optimized the results through fine-tuning in later stages. This validates the effectiveness and stability of the algorithm in handling complex thermodynamic systems, providing a solid theoretical basis for further enhancing the efficiency of industrial thermal processes.

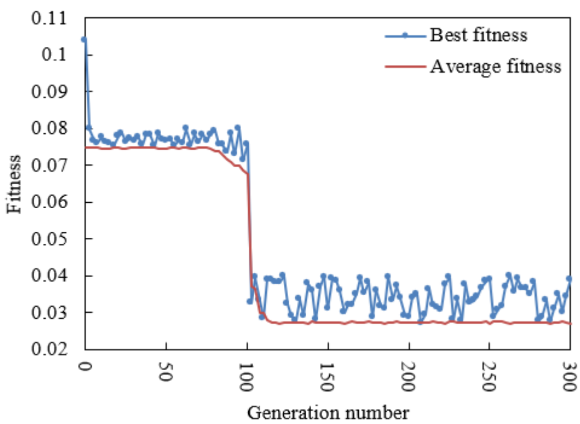

Figure 4. Fitness curve of PSO-optimized Gaussian process regression

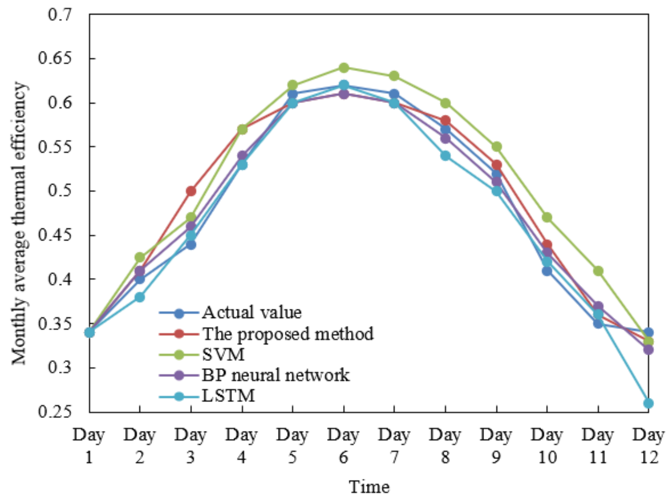

Figure 5. Predictive curves of thermal efficiency for industrial thermal processes by different models

From Figure 5, it is evident that different models vary in their predictive performance for the thermal efficiency of industrial thermal processes. The predictive values of the proposed method are very close to the actual values on most days, especially from day 1 to day 7, where the errors are smaller. After day 7, the predictive values start to deviate slightly, but the overall trend remains consistent with the actual values. In contrast, the SVM model's predictions on day 2, day 3, day 5, and day 6 are higher than the actual values, indicating a tendency to overestimate on these days. The BP neural network's predictions are relatively stable on most days but slightly higher than the actual values from day 10 to day 12. The LSTM model's predictions are close to actual values in the initial phase (day 1 to day 3) but are significantly lower on day 12, indicating that the LSTM model tends to underestimate in long-term predictions. The analysis of the experimental data demonstrates that the proposed method performs excellently in predicting the thermal efficiency of industrial thermal processes, especially in the early and mid-phases, with high accuracy and minimal error. This validates the effectiveness and stability of the optimized Gaussian process regression method, which provides more accurate predictions most of the time compared to other models, showing higher reliability and precision. The SVM and BP neural network models show a certain degree of overestimation on some days, while the LSTM model underestimates in long-term predictions, further highlighting the advantages of the method presented in this paper.

Table 1. Comparison of prediction result errors by different models

Prediction Model	Maximum Relative Error /%	Minimum Relative Error /%	MAPE/%	RMSE/%
The proposed prediction model	7.85	0.03	1.74	0.98
LSTM	6.52	0.22	2.68	1.34
BP neural network	7.58	0.26	5.02	2.89
SVM	10.45	0.31	4.26	2.14

Table 2. Experimental and computational errors in industrial thermal process efficiency

Exhaust Temperature	CO Content in Exhaust	Carbon Content in Slag	Carbon Content in Fly Ash	Received Basis Ash Content	Oxygen Content in Exhaust	Experimental Value	Calculated Value	Relative Error /%
182.2	0.0214	8.56	11.24	1.65	11.24	81.25	81.23	1.14%
214.5	0.0235	12.8	18.95	1.24	8.69	81.23	82.47	1.36%
223.6	0.0124	11.23	22.36	1.62	8.94	81.54	82.31	0.53%
138.5	0.0235	27.54	17.89	1.78	11.24	84.56	84.56	0.36%
171.4	0.0061	3.56	9.56	1.32	13.26	76.25	78.23	1.02%
181.3	0.0124	3.24	3.24	4.25	13.57	75.48	75.14	0.09%
156.2	0.0126	21.56	25.32	1.87	11.25	83.21	83.26	0.65%
172.8	0.0127	11.36	21.47	1.36	12.47	82.45	81.25	1.14%
143.2	0.0412	9.12	16.23	1.89	7.89	89.36	88.48	0.23%
135.6	0.0044	11.47	32.58	2.15	9.56	87.25	89.23	0.12%

From Table 1, it is clear that different models show significant differences in predictive error. The predictive model in this paper has the best performance among all models with a maximum relative error of 7.85%, a minimum relative error of 0.03%, MAPE of 1.74%, and RMSE of 0.98%. Although the LSTM model has the lowest relative error at 6.52% and a minimum relative error of 0.22%, its overall error rates, MAPE of 2.68%, and RMSE of 1.34% are still higher than those of the proposed method. The BP neural network shows poorer performance with a maximum relative error of 7.58%, a minimum relative error of 0.26%, and MAPE and RMSE of 5.02% and 2.89%, respectively. The SVM model exhibits the largest errors with a maximum relative error of 10.45%, a minimum relative error of 0.31%, MAPE of 4.26%, and RMSE of 2.14%. The analysis of the experimental results shows that the method based on optimized Gaussian process regression proposed in this paper significantly outperforms other models in predicting the thermal efficiency of industrial thermal processes. Its error indices are superior to other models, particularly in MAPE and RMSE, indicating high prediction accuracy and stability. In comparison, while the LSTM model has a slight advantage in maximum relative error, its overall errors are still higher than the proposed method, and both the BP neural network and SVM models do not achieve ideal results in error metrics.

From Table 2, it can be seen that the relative errors between experimental values and calculated values are quite small, demonstrating that the proposed method has a high accuracy in predicting the thermal efficiency of industrial thermal processes. Specifically, the relative errors range from 0.09% to 1.36%, with the largest error occurring at an exhaust temperature of 214.5, reaching 1.36%, and the smallest error occurring at an exhaust temperature of 181.3, at 0.09%. Most data points have a relative error below 1%, such as an error of 0.36% at an exhaust temperature of 138.5, and an error of 0.12% at 135.6. These results indicate that the proposed method achieves stable predictive outcomes under various thermodynamic parameters and can accurately reflect actual changes in thermal efficiency. A detailed analysis of the experimental results demonstrates the effectiveness of the thermodynamic foundational research and optimized Gaussian process regression method in improving the prediction of thermal efficiency in industrial thermal processes. The small and stable relative errors indicate that the proposed method performs excellently in handling a variety of thermodynamic factors and process parameters, showing high predictive accuracy and practical value.

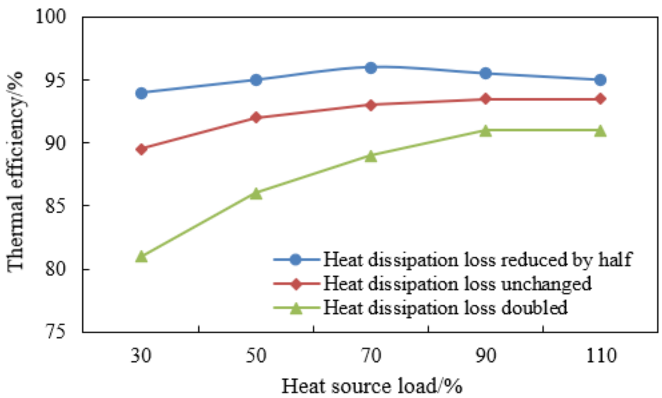

Figure 6. Industrial thermal process efficiency curves under different heat loss conditions

Data from Figure 6 show that the thermal efficiency of the industrial thermal process changes with the heat source load and is significantly influenced by the amount of heat dissipation loss. When the heat dissipation loss is reduced by half, the thermal efficiency remains at a high level, ranging from 94% to 96%, and reaches its highest point of 96% at a heat source load of 70. When the heat dissipation loss is unchanged, the thermal efficiency slightly decreases, ranging from 89.5% to 93.5%, reaching the highest value of 93.5% at a heat source load of 110. However, when the heat dissipation loss is doubled, the thermal efficiency significantly drops, ranging from 81% to 91%, still achieving the highest value of 91% at a heat source load of 110. Analysis of the experimental data shows that reducing heat dissipation loss has a significant effect on improving the thermal efficiency of industrial thermal processes, especially maintaining a high efficiency level under different heat source load conditions. In contrast, when heat dissipation loss increases, the thermal efficiency significantly decreases, further emphasizing the importance of reducing heat dissipation loss.

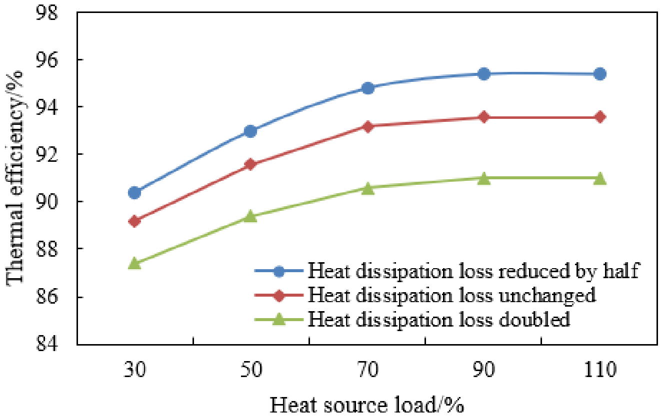

Figure 7. Thermal efficiency curves of industrial thermal processes under different exhaust heat loss conditions

Figure 7 shows that the thermal efficiency of the industrial process varies with heat source load and is significantly affected by exhaust heat loss. When exhaust heat loss is reduced by half, the thermal efficiency remains high under different load conditions, ranging from 90.4% to 95.4%, and reaches its peak at 95.4% at heat source loads of 90 and 110. When exhaust heat loss is unchanged, thermal efficiency slightly declines, ranging from 89.2% to 93.6%, peaking at 93.6% at heat source loads of 90 and 110. However, when exhaust heat loss is doubled, thermal efficiency markedly decreases, ranging from 87.4% to 91%, still peaking at 91% at a heat source load of 110. Analysis of the experimental data shows that reducing exhaust heat loss has a significant effect on enhancing the thermal efficiency of industrial thermal processes, especially maintaining a high efficiency level under different heat source load conditions. In contrast, when exhaust heat loss increases, thermal efficiency significantly decreases, further emphasizing the importance of reducing exhaust heat loss.

The proposed method not only effectively predicted thermal efficiency under different cooling conditions and exhaust heat loss conditions but also provided specific optimization strategies, thereby offering a reliable theoretical foundation and practical guide for energy efficiency improvements in industrial thermal processes, demonstrating their significant value and feasibility in practical applications.

5. CONCLUSION

This paper explored the application of intelligent algorithms in enhancing the efficiency of industrial thermal processes through foundational thermodynamic research, primarily focusing on establishing mathematical models for industrial thermal process efficiency and predicting and optimizing thermal efficiency using optimized Gaussian process regression methods. The experimental results showed that the PSO-optimized Gaussian process regression method performed exceptionally well on the fitness curve, and different models' curves of industrial thermal process efficiency demonstrated the superior performance of the proposed methods in various error metrics. Under different heat dissipation and exhaust heat loss conditions, the methods can effectively predict and optimize thermal efficiency, validating their reliability and effectiveness in practical applications. The results indicated that reducing heat dissipation and exhaust heat loss significantly improved the thermal efficiency of industrial processes, and the proposed methods maintained high predictive accuracy and stability under various load conditions. Specific experimental data revealed that the model's prediction error was significantly lower than other models, with the best performance in maximum relative error, minimum relative error, MAPE, and RMSE, further proving the suitability and superiority of the proposed method under various thermodynamic factors and process parameters.

The research presented in this article provided new theoretical and practical methods for improving the thermal efficiency of industrial processes, with significant engineering application value and academic significance. By combining foundational thermodynamics and optimized intelligent algorithms, the solutions proposed offer new ideas and technical approaches for industrial energy efficiency improvements. However, the research also has limitations. Firstly, the collection of experimental data and the construction of the model are primarily based on specific industrial conditions and may not apply to all industrial environments. Secondly, although the optimized Gaussian process regression method performed excellently in this study, its high computational complexity may limit its application in large-scale industrial systems. Future research directions should include further validating and expanding the applicability of the methods in different industrial settings, simplifying and optimizing the algorithm to enhance computational efficiency, and incorporating more thermodynamic factors and process parameters to improve the comprehensive predictive capability and robustness of the model. Additionally, exploring other advanced intelligent algorithms, such as deep learning and reinforcement learning, could further enhance the thermal efficiency and optimization level of industrial thermal processes.

REFERENCES

[1] Price, C.R., Nimbalkar, S.U., Thirumaran, K., Cresko, J. (2023). Smart manufacturing pathways for industrial decarbonization and thermal process intensification. Smart and Sustainable Manufacturing Systems, 7(1): 41-53.

[2] Rosales-Pérez, J.F., Villarruel-Jaramillo, A., Romero-Ramos, J.A., Pérez-García, M., Cardemil, J.M., Escobar, R. (2023). Hybrid system of photovoltaic and solar thermal technologies for industrial process heat. Energies, 16(5): 2220. https://doi.org/10.3390/en16052220

[3] Ingenhoven, P., Lee, L., Saw, W., Rafique, M.M., Potter, D., Nathan, G.J. (2023). Techno-economic assessment from a transient simulation of a concentrated solar thermal plant to deliver high-temperature industrial

process heat. Renewable and Sustainable Energy Reviews, 185: 113626. https://doi.org/10.1016/j.rser.2023.113626

[4] Kim, Y. B., Park, H., Kim, Y. (2024). An empirical study on thermal efficiency and dusty moisture removal efficiency using enthalpy wheel in industrial waste incineration plant. Applied Thermal Engineering, 248: 123203. https://doi.org/10.1016/j.applthermaleng.2024.123203

[5] Malik, N., Tripathi, S., Aniruddha, R., Babu, V.S., Sreedhar, I. (2022). Strategy to enhance thermal efficiency of evaporators in an industrial jaggery production. Materials Today: Proceedings, 60: 1909-1913. https://doi.org/10.1016/j.matpr.2022.01.006

[6] Anitha, S., Kumar, S.B., Umamaheswari, S., Parthiban, V., Pichumani, M. (2021). Aluminum oxide hydroxide hybrid nanofluids: Do they benchmark thermal efficiency for industrial usage. International Journal of Fluid Mechanics Research, 48(6): 59-71. https://doi.org/10.1615/InterJFluidMechRes.2021040495

[7] Yılmaz, İ., Söylemez, M. (2020). A novel thermal analysis for cooking process in bulgur production: Design considerations, energy efficiency and wastewater diminution for industrial processes. Isı Bilimi ve Tekniği Dergisi, 40(1): 113-129.

[8] Westerholm, M., Castillo, M.D.P., Andersson, A.C., Nilsen, P.J., Schnürer, A. (2019). Effects of thermal hydrolytic pre-treatment on biogas process efficiency and microbial community structure in industrial-and laboratory-scale digesters. Waste Management, 95: 150-160. https://doi.org/10.1016/j.wasman.2019.06.004

[9] Bisht, P.S., Gopalakrishnan, B., Dahal, R., Li, H., Liu, Z. (2024). Parametric energy efficiency impact analysis for industrial process heating furnaces using the manufacturing energy assessment software for utility reduction. Processes, 12(4): 737. https://doi.org/10.3390/pr12040737

[10] dos Santos, G.C., Santos, S.M.D., da Costa Siqueira, M., et al. (2023). The case of the Brazilian Alliance Program: A voluntary energy efficiency agreement based on industrial process analysis. Energy Efficiency, 16(5): 39. https://doi.org/10.1007/s12053-023-10117-5

[11] Zhang, Q., Yi, H., Yu, Z., Gao, J., Wang, X., Lin, H., Shen, B. (2018). Energy-exergy analysis and energy efficiency improvement of coal-fired industrial boilers based on thermal test data. Applied Thermal Engineering, 144: 614-627. https://doi.org/10.1016/j.applthermaleng.2018.08.069

[12] Wang, T., Zhang, H., Zhang, Y., Wang, H., Lyu, J., Yue, G. (2022). Efficiency and emissions of gas-fired industrial boiler fueled with hydrogen-enriched nature gas: A case study of 108 t/h steam boiler. International Journal of Hydrogen Energy, 47(65): 28188-28203. https://doi.org/10.1016/j.ijhydene.2022.06.121

[13] Yuan, P., Guo, T., Pan, X., Hu, X., Ma, J., Xu, D., Zhou, Z., Guo, Q., Guo, X. (2023). Process optimization and thermodynamic analysis of autothermal coal chemical looping gasification industrial demonstration system. Fuel, 334: 126667. https://doi.org/10.1016/j.fuel.2022.126667

[14] Back, S.K., Lee, E.S., Seo, Y.C., Jang, H.N. (2020). The effect of NaOH for the recovery of elemental mercury from simulated mixture wastes and waste sludge from an industrial process using a thermal desorption process. Journal of Hazardous Materials, 384: 121291. https://doi.org/10.1016/j.jhazmat.2019.121291

[15] Kumar, S., Mahavar, S., Mawire, A., Ruivo, C.R. (2023). Design development of an economic solar paraboloidal concentrator for industrial process heat generation. Energy Conversion and Management, 292: 117380. https://doi.org/10.1016/j.enconman.2023.117380

[16] Dsouza, N., Singh, A.K., Maurya, R., Kanakala, R., Madaka, R., Bandaru, N., Uddin, M.S., Rath, J.K. (2023). Silicon surface passivation of industrial n-type CZ Si (111) by Al2O3 layers deposited by thermal ALD process for application in carrier selective contact solar cells. Journal of Materials Science: Materials in Electronics, 34(14): 1179. https://doi.org/10.1007/s10854-023-10587-4

[17] Zhu, G., Zhang, Y., Mishra, R. (2019). Development of a novel methodology for calculating the thermal efficiency of clean fuel boilers based on error analysis method. International Journal of COMADEM, 22(2): 5-9.

[18] Kumar, L., Hasanuzzaman, M., Rahim, N.A., Sleiti, A.K. (2024). Thermoeconomic analysis of a solar-assisted industrial process heating system. International Journal of Energy Research, 2024: 4614066. https://doi.org/10.1155/2024/4614066

[19] Immonen, J., Powell, K.M. (2022). Dynamic optimization with flexible heat integration of a solar parabolic trough collector plant with thermal energy storage used for industrial process heat. Energy Conversion and Management, 267: 115921. https://doi.org/10.1016/j.enconman.2022.115921